

Influence of reduced light speed approximation on reionization fronts speed in cosmological RHD simulations

Nicolas Deparis¹★

¹ *Observatoire Astronomique de Strasbourg, CNRS UMR 7550, Universite de Strasbourg, Strasbourg, France*

Accepted XXX. Received YYY; in original form ZZZ

ABSTRACT

We run a set of radiative hydrodynamic (RHD) cosmological simulations of reionization to explore the link between the ionization rate and the reduced speed of light approximation.

Key words: cosmology: dark ages, reionization, first stars - methods: numerical

1 INTRODUCTION

One fundamental base of numerical simulation is called the Courant-Friedrichs-Lewy (CFL) condition. This condition link the temporal resolution of a numerical experiment to its spatial resolution. The intrinsic link between these two quantity is the velocity of the considered fluid, faster phenomena need more temporal resolution and thus more computational cost. As light is the fastest known phenomena, simulating radiative transfer can be really expensive.

In the aims to reduce this cost, the reduced speed of light approximation was developped.

In a case that the reionization history stay the same with $c=1$ and $c=0.1$, we could gain a factor ten in the computation of radiative processes, wich is really appreciable as radiation represent more than the half of the computational cost in this kind of simulation.

We want to explore how changing the speed of light influence the evolution of ionization fraction during the reionization epoch.

RSLA introduction (Gnedin & Abel 2001; Aubert & Teyssier 2008)

In (Gnedin 2016), the RSLA do not change the reionization history if $c > 0.1$ in $(20 \text{ cMpc/h})^{**3}$ boxes

In (Bauer et al. 2015; Rosdahl et al. 2013), the RSLA significantly change the reionization history, as c decrease, the reionization occurs later.

2 METHODOLOGY

We run our simulations with EMMA an AMR cosmological code with full radiative hydrodynamic (RHD) capability **ref**. We are considering box of a size of $8/h$ cMpc cube from

redshift $z=150$ to $z=5$, resolved with 256^3 dark matter particle on the coarse grid wich lead to a mass resolution of $3.4 \cdot 10^6 M_\odot$ and a spatial resolution of 46 ckpc on the coarse grid. The grid is refined according to a semi-Lagrangian scheme and the refinement is not allowed if the spatial resolution of the newly formed cells is under 500pc. Our stellar mass resolution is set to be equal to $7.2 \cdot 10^4 M_\odot$.

We calibrate our emissivity model using Starburst99, with a $10^6 M_\odot$ population and a $Z=0.001$ metalicity.

We run three simulations with the exact same parameters except that we change the speed of light in the radiative solver.

3 RESULTS

We run three simulations with different reduced speed of light, $c=1$, $c=10\%$ and $c=1\%$ of the real speed of light. We first calibrate the star formation to be in accordance with Bouwens 2015, then we calibrate the emissivity of radiative source using the $c=0.1$ run. We then run $c=1$ and $c=0.01$ simulations without changing any parameters except the speed of light.

3.1 Star formation and ionization histories

We first look at global observable.

On Fig 1a we observe that radiative feedback does not impact star formation histories. Previous work **ref** show that radiative feedback tends to suppress star formation in light halos ($M < 10^9 M_\odot$) but this class of halo do not represent a significant part of the cosmic SFR.

The radiative feedback does not change the cosmic SFR, and thus does not change the ionizing energy budget. So with the same amount of photon, we were expecting that the faster the light is, the sooner the photon could reach the void, and then the sooner the reionization. As always, things

★ E-mail: nicolas.deparis@astro.unistra.fr

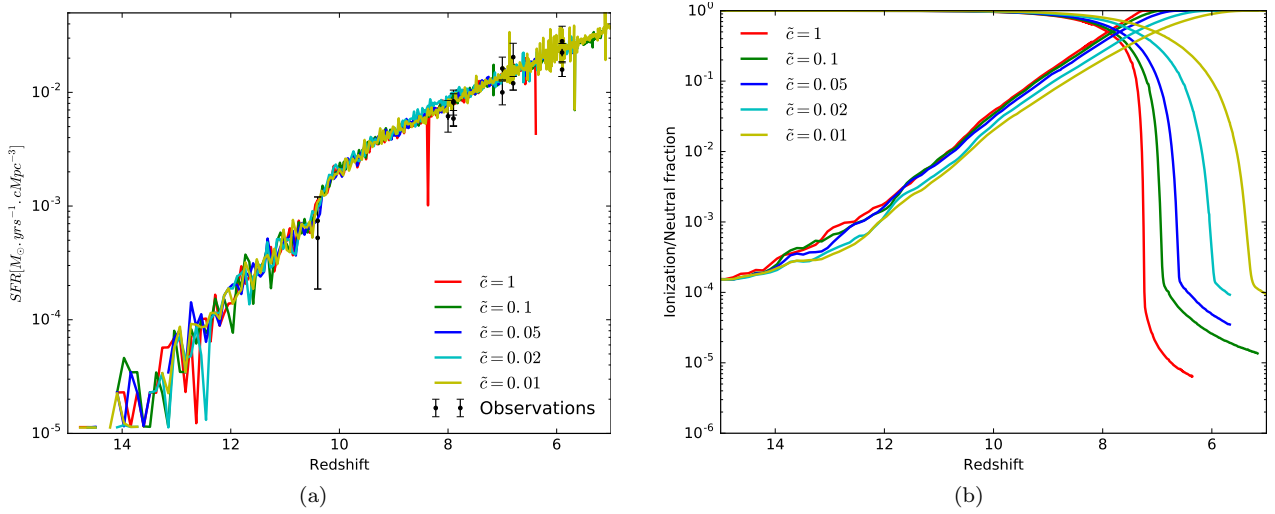


Figure 1. (a) Cosmic star formation histories; (b) volume weighted ionization (solid lines) and neutral (dashed lines) fraction function of redshift for different reduced speed of light. Radiative feedback get almost no impact on the cosmic SFR. But ionization histories are significantly different. We were waiting for slower ionization fronts and so later cosmic reionization with slower RSLA but the behaviour is not that simple.

are not that simple. Fig. 1b presents the average volume weighted ionization state as a function of time :

$$X_V(t) = \frac{\int x(t) \cdot dV}{\int dV}, \quad (1)$$

with the local ionization fraction :

$$x(t) = \frac{n_{H+}}{n_H} \quad (2)$$

Theses curves show that the $c=0.1$ simulation reionize first, then the $c=1$ and finally the $c=0.01$ run. Moreover all simulations see their first stellar particle appear at the same redshift $z \approx 16.2$ but the $c=1$ run see it ionization fraction starting to increase first, then $c=0.01$ and finally $c=0.1$. So the curves order is not conserved through the time.

3.2 Average ionization rate

The average ionization rate $\dot{X}_{(t)}$ is the temporal derivative of the ionization history.

$$\dot{X}_{(t)} = V_{box} \frac{\partial X_{(t)}}{\partial t} = [\text{ckpc}^3 \cdot \text{yr}^{-1}], \quad (3)$$

where V_{box} represent the simulated volume in ckpc^3 .

Fig. 2 present the average volume weighted ionization rate for our three simulations.

The maximum rate is obtained just before the reionization end, where bubble are collapsing in the void. We observe that the faster the light is, the higher the maximum ionization rate.

The $c=0.1$ and $c=0.01$ curve have a exponential increase of the ionization rate from the apparition of the first star to $z \approx 8$. The $c=1$ curve present two regime at high redshift: the ionization rate slowly increase until $z \approx 11$ where the curve became steeper to get a comparable slope to the one of the two others runs.

An other way to look at the ionization rate is to consider the ability of newly formed stars to ionized their environment. This can be achieve by dividing the ionization rate history $\dot{X}_{(t)}$ by the star formation history $\dot{\rho}_{(t)}^*$.

$$\dot{X}_{(\rho^*)} = \frac{\dot{X}_{(t)}}{\dot{\rho}_{(t)}^* \cdot V_{box}} = [\text{ckpc}^3 \cdot \text{M}_{\odot}^{-1}] \quad (4)$$

The resulting computation is presented on Fig. 2b. For the $c1$ run (in red) and before redshift $z=11$, newly formed stars tend to lose in ability to ionize their environment.

If first forming stars get a high speed light ($c=1$), their radiative feedback could reach region further than in the reduced light speed case. Radiative feedback is able to reduce SFR in low mass halos, and at high redshift high mass halos has no time to form. From these hypothesis, we could imagine that in the $c=1$ case, early radiative can reach surrounding low masses halo, and cut down their star formation.

From this plot we conclude that this is not a mater of direct early feedback but that early sources tend to lose their ability to ionized the medium in the first time (before $z=11$) and then this ability significantly increase.

3.3 Ionization maps

For each cell, we keep in memory the time where its ionization fraction pass a given threshold.

The computation is done during simulation runtime, and due to the AMR property of the grid we choose to work with time and not with redshift. Indeed, when cells have to be de-refined, the value of each eight leaf cells have to be propagated to their mother. This action generally consist into averaging these eight values. As physical processes governing the ionization state are computed in time space, it seems *a priori* more reasonable to average time value than redshift. At the end of the simulation, where the reionization is done, the AMR reionization-time grid is projected

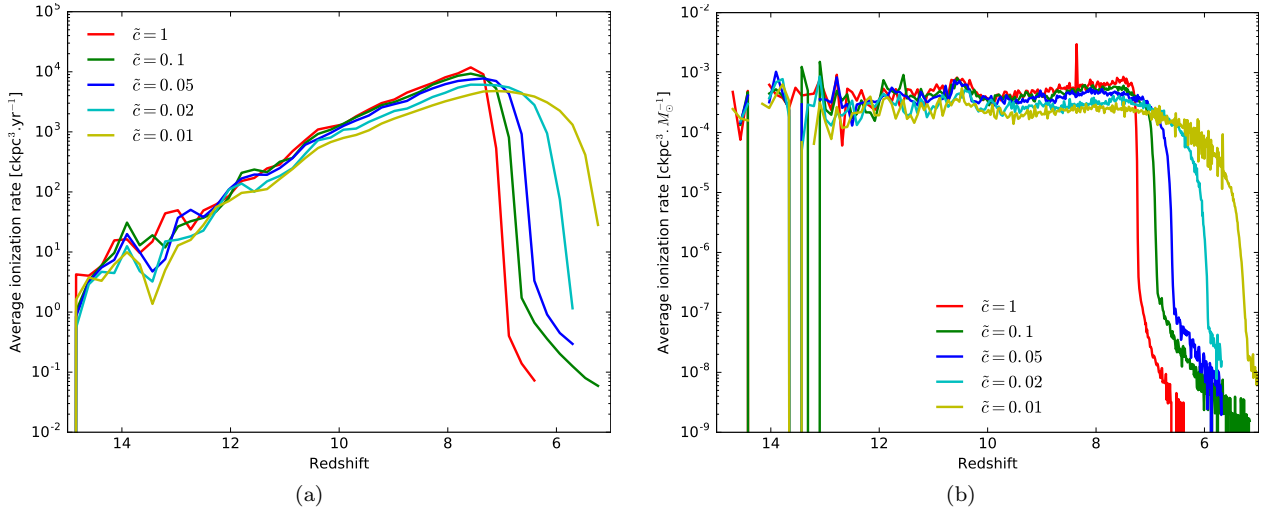


Figure 2. Average ionization rate time weighted (a) and stellar mass weighted (b) function of redshift for different speed of light.

on a regular grid at the base level resolution. Finally this reionization time cube is converted into a redshift time cube using standard cosmology integration.

It is possible to choose to keep the first or the last reionization time. The difference between first and last ionization maps will be significant in dense region where recombination can be high but will globally be the same in void who do not recombine. As under dense region represent the major part of the volume, the volume weighted ionization state is mostly governed by void

In this study, the reionization time is considered to be the last time where the volume weighted ionization fraction pass through 50%.

Fig. 5 shows three maps of reionization redshift for our three run. Those maps are one cells thick slices taken at the same coordinate in the z axis for the three maps. The z is chosen to contain the first cell to pass the threshold in the $c=0.1$ simulation.

The global behaviour is similar between runs. The sources are at the same place independently of the run, which is coherent with the fact that the ionizing feedback do not significantly change global star formation processes in our simulation (Fig 1a). Radiation leaves high density regions in comparable butterfly shapes.

Light takes time to reach the voids, so voids are associated to lower reionization redshift. In the $c=0.01$ map the $5 < z < 6$ redshift range (in blue shade) represent the void, the same region in the $c=0.1$ run is reionized sooner and correspond to a reionization redshift of $z \approx 7$ (in green). But the same region in the $c=1$ run is reionized later than in the $c=0.01$ run in the $6 < z < 7$ redshift range (transition between green and blue)

This is correlated to what we observe in Fig. 1b, $c=0.1$ run reionize first because its void reionize at higher redshift

Fig. 5 also shows the probability density function of reionization redshift taken in the whole volume for our three simulations.

At high redshift ($z > 10$) the reionization redshift PDF is dominated by low light velocity.

For the three runs, the most probable redshift is in the

range $8 > z > 6$, but the maximum probability increase with the speed of light withch is a similar behavior to what we observe in the ionization rate curve (Fig. 2b)

It seems the the delay taken by the $c=1$ run at high redshift can't catch again at lower redshift, where

3.4 Ionization fronts speeds

The reionization maps represent a time at each point of the space. The spatial gradient of this map, contain the information of the direction and the speed of the ionization front. The gradient represent the time needed to ionize a given distance, in $[\text{yr.pc}^{-1}]$. The reverse of this gradient can then be interpreted as a velocity (in $[\text{pc.yr}^{-1}]$).

We define the reionization front speed V_{reio} as :

$$V_{reio} = \left| \frac{1}{\vec{\nabla} t_{reio}} \right|. \quad (5)$$

As we want to compared this speed to the speed of light, we want it in physical units (as opposed as comoving units). So the gradient of a cell i is weighted by a^i the scale factor of the cell at its reionization time.

$$\vec{\nabla} t_{reio}^i \approx \frac{t^{i+1} - t^{i-1}}{2a^i (x^{i+1} - x^{i-1})} \quad (6)$$

This map correspond to the velocity of the ionizing front. Analysing this velocity as a function of the considered reduce light speed can help simulator to understand how important is the speed of light in simulation.

- Convert reionization redshift into reionization time
- Take the gradient of the reionization time
- invert this gradient to get a speed

Fig. 4 shows maps of reionization speed for our three run with different reduced speed of light.

Maximums values are located either near the sources or in the void. Nears the sources, the photon budget is high, but the medium is dense at the recombination rate is also

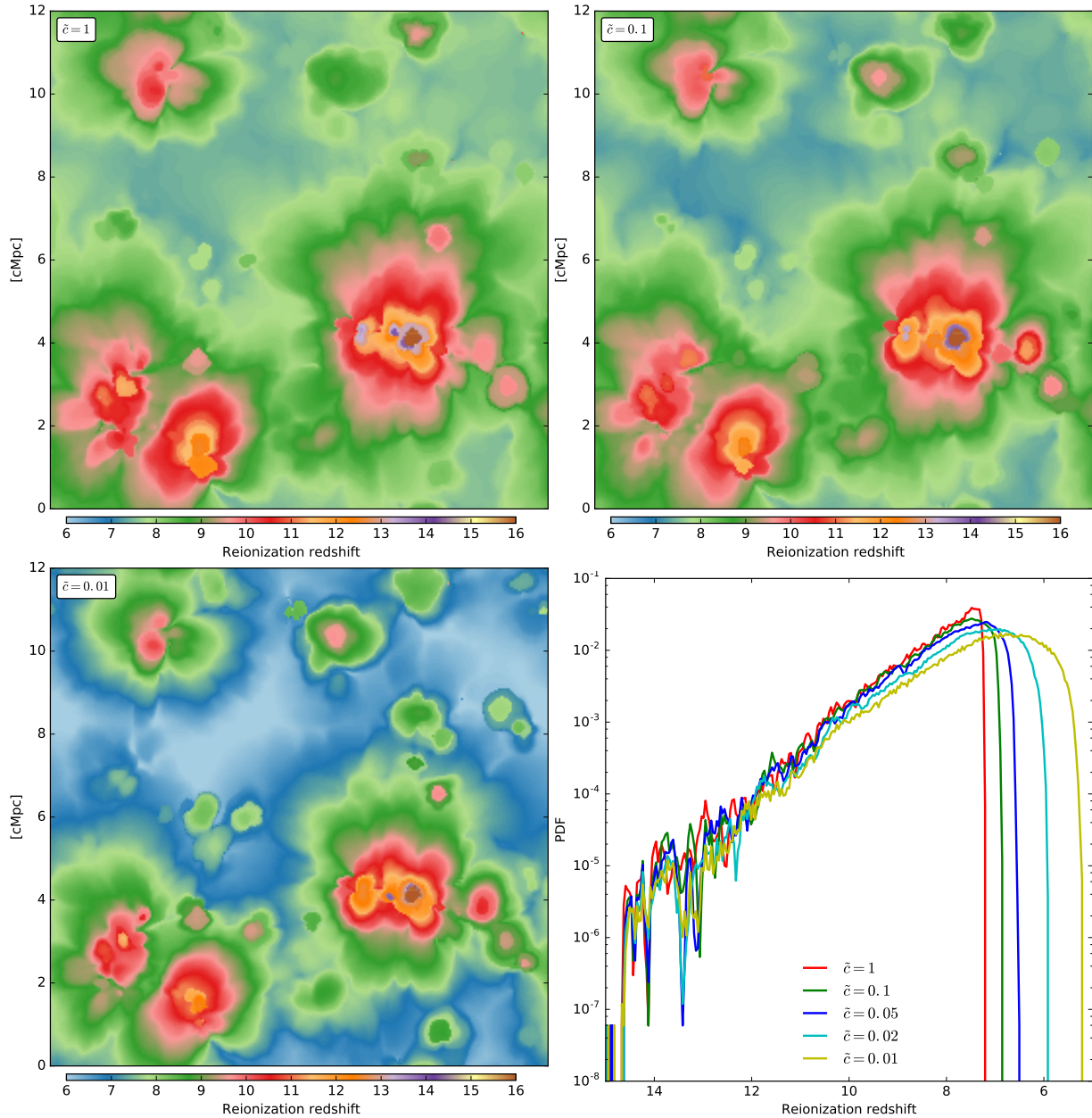


Figure 3. Maps and PDF of reionization redshift for runs with different reduced speed of light.

high. In the void there is less photon but the drop in the density compensate it.

Reionization speed can be greater than the speed of light in the simulation, up to several time. The limit case is when two neighbouring cells reionize at the same timestep, their gradient became null and the associated reionization speed became infinite. This can happen in two cases:

- In over-dense regions, where two adjacent cells form stars at the same time and instantaneously reionized.
- In under-dense regions, during the collapse of two ionization fronts.

This part of spurious speed represent a small fraction of the volume (with a volume proportion of $8 \cdot 10^{-5}$ in the worst case).

There is a concentric behaviour. Near the sources the

ionization front speed is high and tends to be close to the speed of light. Going further from sources the front velocity quickly drop, which draw that concentric dark shade around star formation site. Reionization fronts consecutively accelerate and decelerate depending on the star formation histories of over densities.

Near the sources, the distance between two low velocities isocontours is linked to the product between the front speed with the radiative life time of internal source. (front is moving forward while source is on) After the source life time ionization front can't goes further and its growth is stopped until the next generation of stars.

A typical value for reionization front speed is about 3000 km.s^{-1} or $10^{-2} c$ (Gnedin 2016)

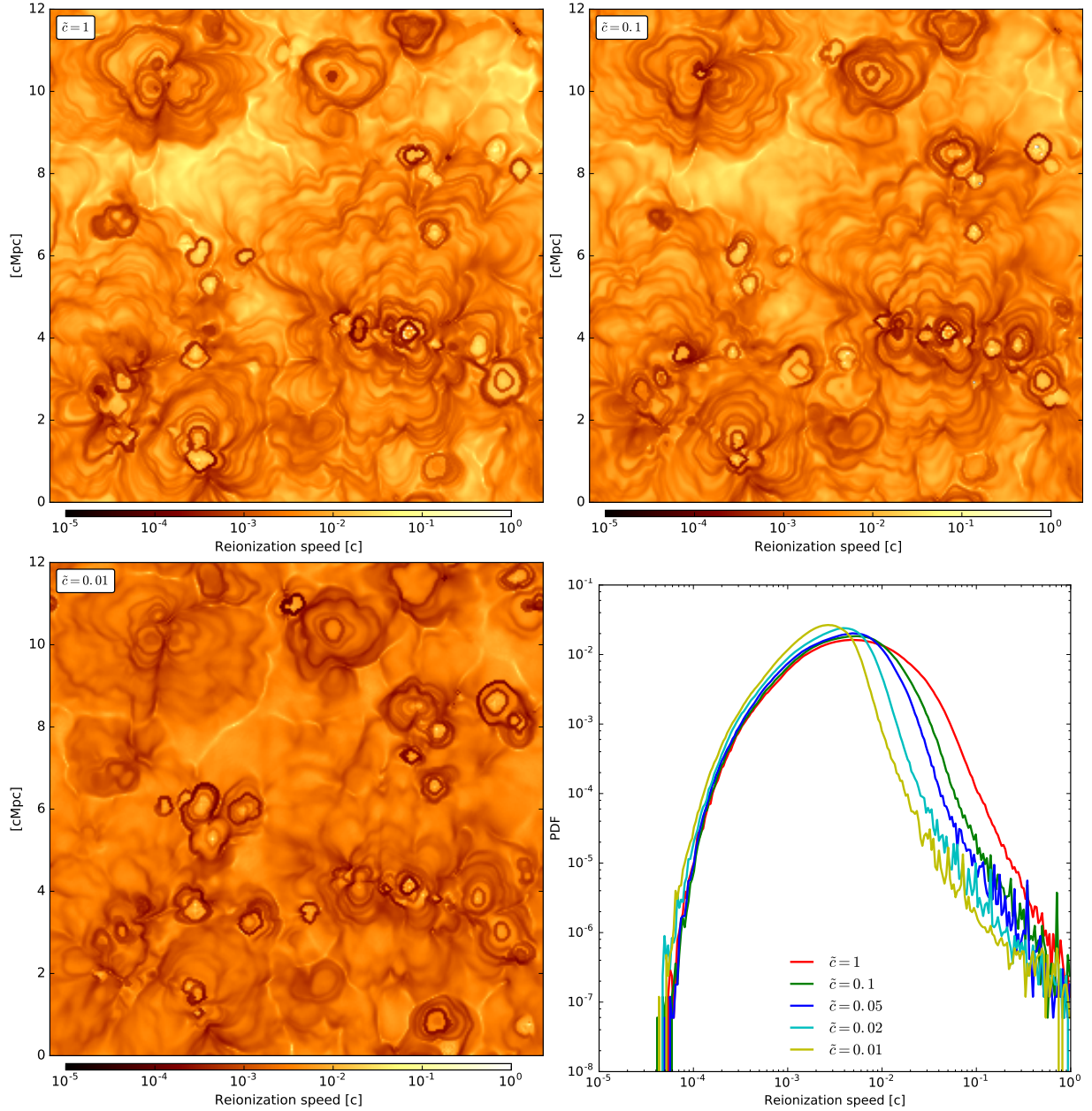


Figure 4. Maps and PDF of reionization front speed for runs with different reduced speed of light approximations. Front speed are expressed relatively to the real speed of light.

3.5 Speed of ionization fronts as a function of redshift

We have associated a redshift and a speed at each point of space. We now look at the evolution of the reionization speed as a function of redshift.

Looking in decreasing redshift:

High redshift non zero front speed tends to appear later with higher light speed. For instance, the $z > 12$ part of the $c=1$ histogram is almost void, while the same part of the $c=0.01$ histogram is populated. The reionization start sooner with lower speed of light.

Reducing the speed of light in the simulation limit the probability to find a front speed above this limit. At redshift $z=6$, increasing the speed of light creates a peak in the

distribution, the height of this peak is linked to the setup speed value. With an high speed of light the box flash faster at the end of the reionization the with lower value.

After the reionization, where ionization bubbles has collapse, the probability to find an high speed front drop suddenly. But high light speeds leave a residual bulge of non zeros, low velocities front after this drop.

4 DISCUSSIONS AND CONCLUSION

ACKNOWLEDGEMENTS

This work is supported by the ANR ORAGE grant ANR-14-CE33-0016 of the French Agence Nationale de la Recherche.

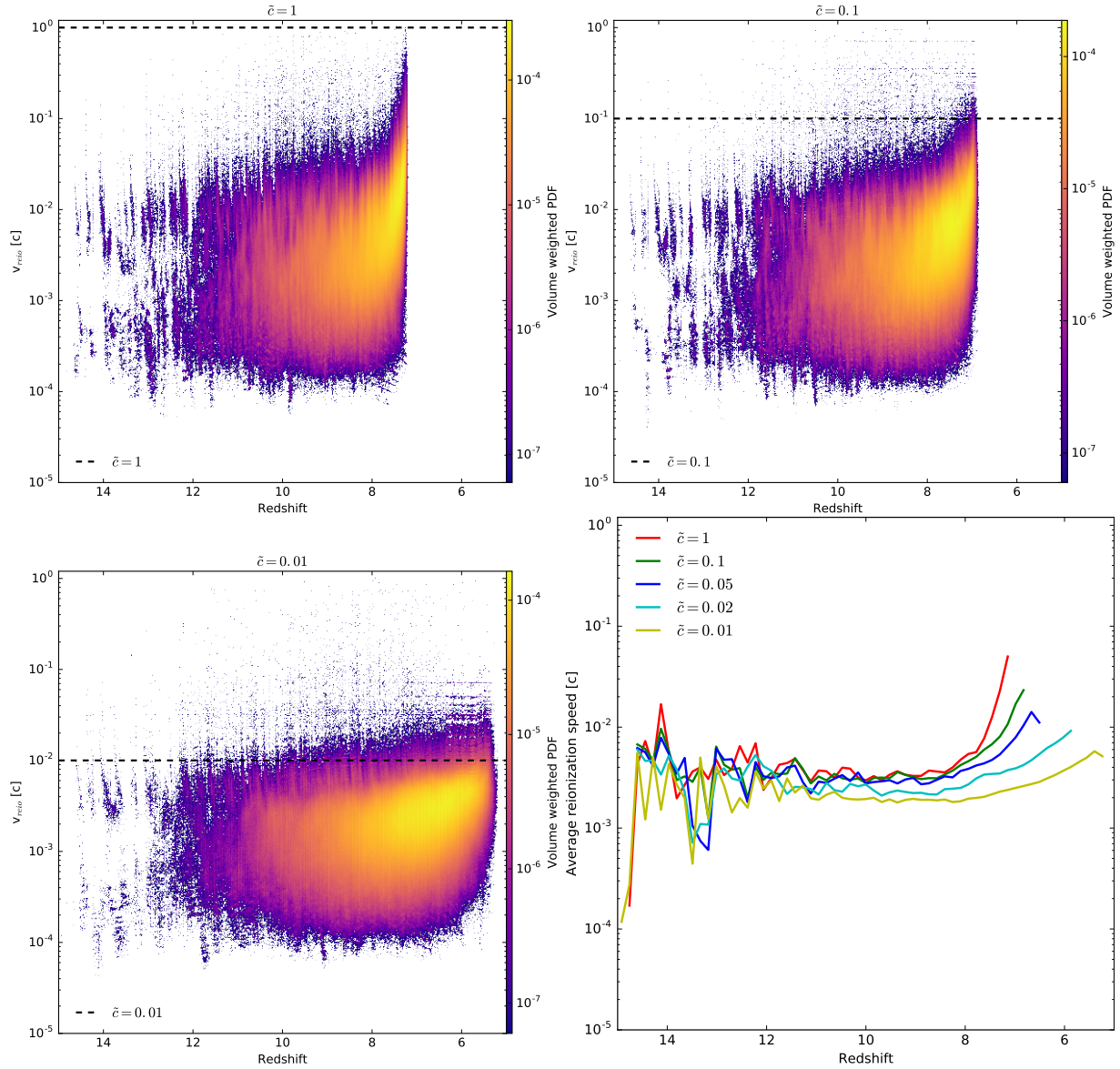


Figure 5. 2d histogram of reionization speed in unit of the real speed of light as a function of redshift for different reduced light speed RSLA. The horizontal dashed line represents the light speed in the simulation. And averaged reionization speed as a function of redshift.

REFERENCES

- Aubert D., Teyssier R., 2008, *Monthly Notices of the Royal Astronomical Society*, 387, 295
 Bauer A., Springel V., Vogelsberger M., Genel S., Torrey P., Sijacki D., Nelson D., Hernquist L., 2015, *Monthly Notices of the Royal Astronomical Society*, 453, 3593
 Gnedin N. Y., 2016, *The Astrophysical Journal*, 833, 66
 Gnedin N. Y., Abel T., 2001, *New Astronomy*, 6, 437
 Rosdahl J., Blaizot J., Aubert D., Stranex T., Teyssier R., 2013, *Monthly Notices of the Royal Astronomical Society*, 436, 2188

This paper has been typeset from a \LaTeX file prepared by the author.